InAsSb/InAs: A type-I or a type-II band alignment

Su-Huai Wei and Alex Zunger
National Renewable Energy Laboratory, Golden, Colorado 80401
(Received 14 June 1995)

Using first-principles band-structure calculations we have studied the valence-band alignment of InAs/InSb, deducing also the offset at the $InAs_{1-x}Sb_x/InAs_{1-y}Sb_y$ heterostructure. We find the following: (i) Pure InAs/InSb has a "type-II broken gap" alignment both with and without strain. (ii) For Sb-rich $InAs_{1-x}Sb_x$/InSb heterostructures, the unstrained band alignment is type II; both epitaxial strain and CuPt ordering enhance the type-II character in this Sb-rich limit. (iii) For As-rich $InAs/InAs_{1-x}Sb_x$ heterostructures the top of the valence band is always on the alloy layer while the conduction-band minimum can be localized either on the alloy layer (type-I) or on the InAs layer (type-II), depending on the balance between concentration, strain, and degree of ordering/phase separation. In this case, epitaxial strain enhances the type-II character, while ordering enhances the type-I character. Our results are compared with recent experimental observations. We find that the type-I behavior noted for some As-rich $InAs/InAs_{1-x}Sb_x$ interfaces and the type-II behavior noted in other such samples could be explained in terms of the dominance of ordering and strain effects, respectively.

I. INTRODUCTION

$InAs_{1-x}Sb_x/InAs_{1-y}Sb_y$ semiconductor alloys and heterojunctions have been studied as potential IR detectors and emitters[1-12]. While the $InAs_{1-x}Sb_x$ alloy system provides the lowest band gap attainable within the family of bulk III-V semiconductors [145 meV at $x=0.634$ (Ref. 13)], this value is not small enough to produce the $10-12\mu$ absorption (124–103 meV) needed in far-infrared detection. Two strategies present themselves: one can either change the growth conditions to promote CuPt ordering of the $InAs_{1-x}Sb_x$ alloy,[4,5] thus reducing its band gap.[4] Alternatively, one can form a heterojunction between an arsenide-rich and an antimonide-rich alloy with a *type-II band alignment,* in which case the effective band gap is smaller than either of the constituents. The latter approach has been proposed[1] and tested[2,3] for *Sb-rich* heterojunctions. The $InAs_{0.13}Sb_{0.87}$/InSb strained-layer superlattices, for example, was found to have a type-II band alignment, with a valence-band maximum (VBM) on the InSb layer and a conduction-band minimum (CBM) on the alloy layer. The estimated[2,3] unstrained valence-band offset ΔE_v(InAs/InSb) was about 400 meV. Recently, interest in developing midinfrared lasers and detectors has lead to growth and characterization of the opposite limit of *As-rich* $InAs_{1-x}Sb_x/InAs$ superlattices.[6-12] However, in this case, experimental results for the type (I or II) of band alignment are conflicting.

(i) Metal-organic chemical-vapor deposition (MOCVD)- grown $InAs_{1-x}Sb_x/InAs$ ($x\sim0.1$) strained-layer superlattices and quantum wells reported by the Sandia group[6-8] exhibited a large electron quantum confinement spectral shift and a decrease in the hole effective mass in magnetophotoluminescence, suggesting that both the electrons and holes are confined to the *alloy* layer, thus a type-I band alignment [Fig. 1(a)].

(ii) Molecular-beam-epitaxy (MBE)-grown $InAs_{1-x}Sb_x/InAs$ ($x\sim0.1-0.4$) strained-layer superlattices reported in Refs. 9 and 10 by the Imperial College group were analyzed in terms of photoluminescence (PL) and magnetotransmission. The PL spectra showed emission energies lower than the band gaps of either of the superlattice components, suggesting a type-II band alignment. Fitting one or two PL energies per sample to a

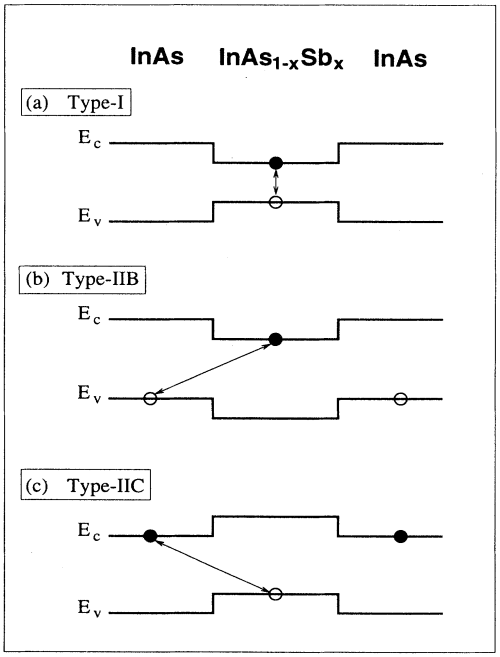

FIG. 1. Schematic plot of the possible band alignments discussed in this paper. The solid arrows denote the lowest band gap.

Kronig-Penney model was used to extract values of the band offset. The best fit (to two emission lines) corresponded to a band arrangement shown in Fig. 1(b) with electrons in $InAs_{1-x}Sb_x$ layer and holes in the InAs layer. The extrapolated unstrained valence-band offset was $\Delta E_v(\text{InAs/InSb}) = -840$ meV (note the negative sign denoting the VBM of InAs is *higher* than that of InSb). This type-IIB band alignment was further supported by their magnetotransmission data,[9,10] where an envelope-function fit to six interband transitions showed that the absorption line *below* the PL energy had a much larger mass than usual. This suggested to the authors that the lowest transition was related to the light hole in the InAs layer, thus $\Delta E_v < 0$. These researchers have also considered[10] a type-IIC band alignment [Fig. 1(c)] with electrons on the InAs and holes on the $InAs_{1-x}Sb_x$ alloy ($\Delta E_v > 0$), but concluded that the magnetotransmission data (and the two-peak PL data) better supported the type-IIB $\Delta E_v < 0$ assignment.

(iii) The MBE-grown $InAs_{1-x}Sb_x$/InAs ($x = 0.07$) laser structure reported in Refs. 11 and 12 by the Hughes group were modeled by the Kronig-Penney approach, assuming a type-IIC [Fig. 1(c)] band alignment. The computed emission wavelength agreed reasonably well with the measured value, assuming literature values of the unstrained band offsets of $\Delta E_v(\text{InAs/InSb}) = 610$ meV (Ref. 14) or $\Delta E_v(\text{InAs/InSb}) = 410$ meV.[2(b)] However, these values were not directly measured;[2,3,14] they were inferred instead from simple model fits of alloy heterojunctions (Sb-rich InAsSb/InSb in Refs. 2 and 3, and GaInSb/InAs in Ref. 14), and extrapolated to the pure unstrained InAs/InSb components. Given the uncertainty in the input values (e.g., ΔE_v) used by Zhang and coworkers,[11,12] and given that the resulting conduction-band offset was very small (~ 11 meV), it is difficult to establish if the system is type I or II.

Given the diverging views on the type of InAs/InSb band offsets needed to explain the data [type-I with $\Delta E_v > 0$;[6-8] type IIB with $\Delta E_v < 0$,[9,10] or type IIC with $\Delta E_v > 0$;[11,12] see Fig. 1], a *direct core-photoemission measurement* would be highly desirable. Indeed, extracting indirectly a value of the unstrained band offset by fitting emission or absorption energies can depend sensitively both on the type of model used, and on the precise values of the other parameters, including masses and deformation potentials. Here we report a first-principles calculation of the heterojunction band offset as a function of composition and strain and propose a possible explanation for the above-stated conflicting results.

We note at the outset that the suggestion[9,10] that the Sb VBM is (~ 840 meV) *lower* than the As VBM (i.e., that $\Delta E_v < 0$) conflicts with all previously known *calculations* of the As/Sb band offsets: The model solid approach of Van de Walle yielded[15] $\Delta E_v(\text{InAs/InSb}) = +720$ meV, and the model of Qteish and Needs yielded[16] $+650$ meV. Similarly, first-principles local-density-approximation (LDA) calculations by Wei and Zunger yielded[17] ΔE_v (GaAs/GaSb) $= +650$ meV for a related As/Sb interface, while experimental results[18] on this system also yield $\Delta E_v \gg 0$. Thus there appears to be some doubt whether model IIB ($\Delta E_v < 0$) is appropriate for an intrinsic As/Sb heterojunction. More on this below.

II. METHOD OF CALCULATION OF BAND OFFSET BETWEEN STRAINED BINARIES

We first calculate the valence-band offsets directly as a function of strain for the binaries InAs/InSb using the first-principles local-density-functional formalism,[19-21] as implemented by the all-electron general potential, relativistic, linearized augmented-plane-wave (LAPW) method.[22] The method of calculation of the band offset is described in detail elsewhere;[23] it parallels its measurement via core photoemission. The valence-band offset between two materials AC and AD is expressed as

$$\Delta E_v(AD/AC) = \Delta E^{AC}_{\text{VBM,core}} - \Delta E^{AD}_{\text{VBM,core}} + \Delta E_{\text{core}} . \quad (1)$$

[In this expression, a positive $\Delta E_v(AD/AC)$ value means that the VBM is higher on the AC compound.] Here, $\Delta E^{AC}_{\text{VBM,core}} = E^{AC}_{\text{VBM}} - E^{AC}_{\text{core}}$ and $\Delta E^{AD}_{\text{VBM,core}} = E^{AD}_{\text{VBM}} - E^{AD}_{\text{core}}$ are the energy separations between the core level and the VBM for materials AC and AD, respectively, and $\Delta E_{\text{core}} = E^{AC}_{\text{core}} - E^{AD}_{\text{core}}$ is the difference in core-level orbital energies between AC and AD on each side of the heterojunction. To obtain the unstrained band offset, the first two terms in Eq. (1) are calculated using the cubic equilibrium lattice constants of the isolated constituents AC and AD, while the third term is determined using a (001) $(AC)_n/(AD)_n$ superlattice (including its interfacial strain) calculated at the average lattice constant $\bar{a} = \frac{1}{2}[a(\text{InAs}) + a(\text{InSb})]$. Because it is a deep core-level difference, ΔE_{core} is rather insensitive to the choice of superlattice period n, layer orientation, and strain configuration used in the calculation. To obtain the (001) biaxially strained band offsets as a function of the substrate lattice constant a_s, all three terms in Eq. (1) are calculated at the same a_s, with the tetragonal deformation in the perpendicular direction determined by minimizing the total energy. No input on the deformation potential is needed.

LDA calculations are well known[21] to underestimate the band gaps. In the case of materials with narrow gaps (InAs, InSb) the LDA produces even *negative* band gaps. One might wonder to what extent can this LDA *band-gap* error affect the calculated *valence-band offset*. *First,* note that the error in the *valence-band* energy level reflects in part, the indirect error in the calculated LDA total charge density. The latter stems from the fact that some conduction states are erroneously occupied and some valence states are erroneously emptied when $E_g^{\text{LDA}} < 0$ despite $E_g^{\text{expt}} > 0$. However, for direct-gap material, the LDA negative gap occurs only for a single band and strictly only at the immediate vicinity of the Γ point in the Brillouin zone. Hence the error in the *total* charge density is negligible. *Second,* because of symmetry considerations, the valence and conduction bands at the Γ point cannot mix, so the LDA error there is inconsequential as far as band coupling is concerned. In fact, our previous calculation[17] on GaSb gave a very good lat-

tice constant, bulk modulus, and band-gap deformation potential despite $E_g^{\mathrm{LDA}}<0$ and $E_g^{\mathrm{expt}}>0$. Furthermore. to obtain the conduction-band offset under different strain conditions we use the relation $\Delta E_c=\Delta E_g-\Delta E_v$, where $\Delta E_g=E_g^{AC}(\epsilon)-E_g^{AD}(\epsilon)$ is the strain-dependent LDA-corrected band-gap difference between $AD=$InAs and $AC=$InSb. The band gap $E_g(\epsilon)$ for compound AC and strain ϵ is given by

$$E_g^{AC}(\epsilon)=E_{g,\mathrm{LDA}}^{AC}(\epsilon)+[E_{g,\mathrm{expt}}^{AC}(0)-E_{g,\mathrm{LDA}}^{AC}(0)]\ , \qquad (2)$$

where, $E_{g,\mathrm{LDA}}^{AC}(\epsilon)$ is the LDA calculated band gap for compound AC under strain ϵ, and $E_{g,\mathrm{expt}}^{AC}(0)$ is the *experimentally measured*[13] zero-strain band gap at $T=0$. We assume that the LDA *correction* [terms in the square bracket of Eq. (2)] is strain independent. For InAs the LDA correction is 1.11 eV, while for InSb it is 1.00 eV. This method of band-offset calculation has been used in the past to compute the unrelaxed valence-band offsets of numerous semiconductor heterojunctions,[17,23] yielding reasonable agreement with experiment, e.g.,

$$\begin{aligned}
&\Delta E_v(\mathrm{CdTe/HgTe})=0.37\ \mathrm{eV}\ ,\\
&\Delta E_v(\mathrm{ZnTe/HgTe})=0.26\ \mathrm{eV}\ ,\\
&\Delta E_v(\mathrm{CdTe/ZnTe})=0.13\ \mathrm{eV}\ ,\\
&\Delta E_v(\mathrm{MnTe/CdTe})=0.25\ \mathrm{eV}\ ,\\
&\Delta E_v(\mathrm{AlAs/GaAs})=0.42\ \mathrm{eV}\ ,\\
&\Delta E_v(\mathrm{GaAs/GaSb})=0.65\ \mathrm{eV}\ ,\\
&\Delta E_v(\mathrm{ZnS/ZnSe})=0.53\ \mathrm{eV}\ ,\\
&\Delta E_v(\mathrm{ZnSe/ZnTe})=0.73\ \mathrm{eV}\ ,\\
&\Delta E_v(\mathrm{ZnS/ZnTe})=1.26\ \mathrm{eV}\ ,\\
&\Delta E_v(\mathrm{GaP/InP})=0.09\ \mathrm{eV}\ .
\end{aligned} \qquad (3)$$

III. METHOD OF CALCULATION OF BAND OFFSET BETWEEN ALLOY CONSTITUENTS

So far we explained the method of calculating band offsets between the *binary* constituents. To obtain the valence-band offset between alloy constituents $\mathrm{InAs}_{1-x}\mathrm{Sb}_x/\mathrm{InAs}_{1-y}\mathrm{Sb}_y$, we assume that at a given substrate with lattice constant a_s, the valence-band energy varies with composition x as

$$E_v(a_s,x)=E_v(a_s,0)+x\Delta E_v(a_s,\mathrm{InAs/InSb})-b_v x(1-x)\ . \qquad (4)$$

Here $\Delta E_v(a_s,$ InAs/InSb) is our LDA calculated valence-band offset between the *pure* binaries (Sec. II), strained on the substrate with lattice constant a_s. The coefficient b_v is the bowing parameter of the top of the alloy valence band. In general, b_v is negative and its magnitude is much smaller than the total band-gap bowing b_g. The valence-band offset between $\mathrm{InAs}_{1-x}\mathrm{Sb}_x$ and $\mathrm{InAs}_{1-y}\mathrm{Sb}_y$ is $\Delta E_v(a_s,x/y)=E_v(a_s,y)-E_v(a_s,x)$, which can be obtained from Eq. (4). Similarly, for the conduction band we assume

$$E_c(a_s,x)=E_c(a_s,0)+x\Delta E_c(a_s,\mathrm{InAs/InSb})-b_c x(1-x)\ . \qquad (5)$$

Here $\Delta E_c(a_s,\mathrm{InAs/InSb})$ is our LDA-corrected, directly calculated conduction-band offset between the *pure* binaries strained on substrate with lattice constant a_s, and the coefficient $b_c=b_g+b_v$ is the bowing parameter of the CBM.

IV. RESULTS AND DISCUSSIONS

Our results for the band offset between a *pure* InAs/InSb interface in a range of substrates is given in Fig. 2, while the results for the alloy interfaces are shown in Fig. 3. We conclude the following.

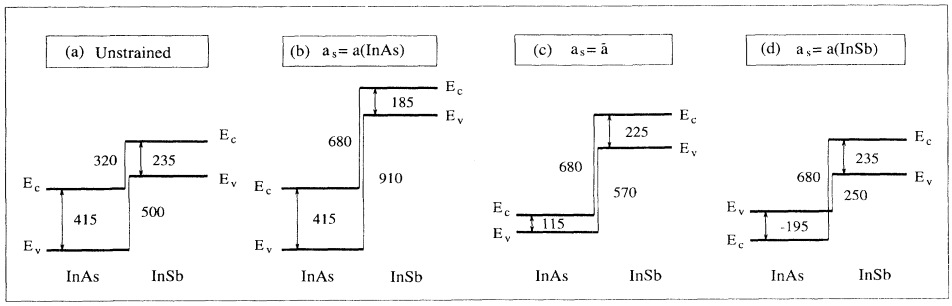

FIG. 2. Calculated band offsets vs strain for pure InAs/InSb heterostructures. Energies are in meV. Only the highest valence state is shown in each case. The InSb-derived lh $(\frac{3}{2},\pm\frac{1}{2})$ state is located at 0, 360, 222, and 0 meV below the VBM for cases (a), (b), (c), and (d), respectively, while the InAs-derived hh $(\frac{3}{2},\pm\frac{3}{2})$ state is located at 0, 0, 259, and 501 meV below the VBM, respectively. The calculated InSb-derived spin-orbit split-off $(\frac{1}{2},\pm\frac{1}{2})$ state is located at 760, 919, 778, and 760 meV below the VBM for cases (a), (b), (c), and (d), respectively, while the calculated InAs-derived spin-orbit split-off $(\frac{1}{2},\pm\frac{1}{2})$ state is located at 372, 372, 452 and 545 meV below the VBM, respectively.

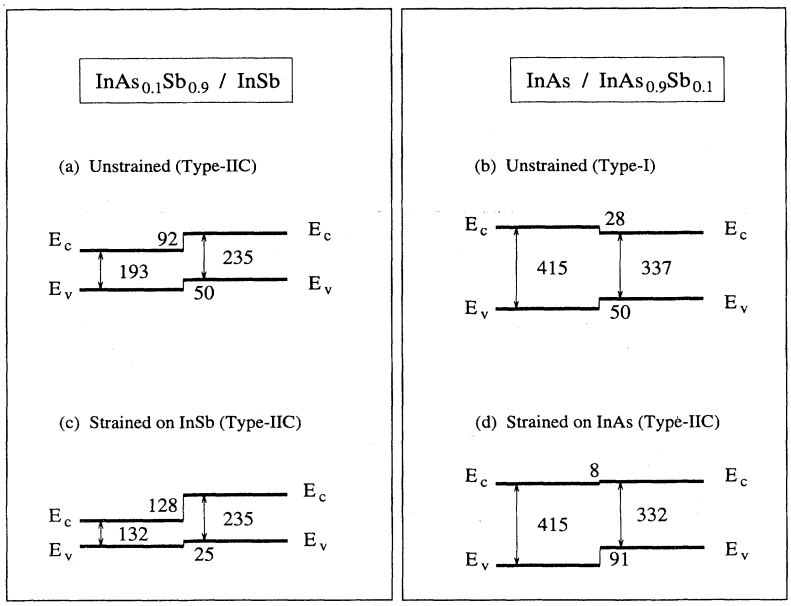

FIG. 3. Calculated band offsets for unstrained (a) and strained (c) $InAs_{0.1}Sb_{0.9}/InSb$ heterostructures; and unstrained (b) and strained (d) $InAs/InAs_{0.9}Sb_{0.1}$ heterostructures. Energies are in meV.

A. Unstrained offsets

The band alignment of pure, unstrained InAs/InSb [Fig. 2(a)] is type-II broken gap, with the CBM of InAs below the VBM of InSb. The calculated unstrained valence-band offset $\Delta E_v = +500$ meV is in reasonably good agreement with previous, less detailed calculations,[15,16] and with experimental estimate,[2,3,14,24] but is in contradiction to the results $\Delta E_v(\text{InAs/InSb}) = -840$ meV obtained from the fit of magnetotransmission and PL data.[9,10] We believe that the negative offset is physically incorrect. This casts doubt on the reliability of the widely used procedure of extracting band offsets from fitting a few absorption/emission lines to an approximate effective mass model, even if the fit quality is good.

B. Effects of alloying in unstrained alloys

Figure 3 depicts results of our calculated unstrained band offset for $InAs_{0.1}Sb_{0.9}/InSb$ [Fig. 3(a)] and for $InAs/InAs_{0.9}Sb_{0.1}$ [Fig. 3(b)]. These results are obtained by using our calculated unstrained valence-band offset $\Delta E_v = 500$ meV and the LDA-corrected conduction-band offset $\Delta E_c = 320$ meV [Fig. 2(a)] in Eqs. (4) and (5), and by attributing all of the measured[13] band-gap optical bowing $b_g = 672$ meV to the conduction band.[25,26] [Our input data are hence $b_v = 0$, $b_c = b_g = 672$ meV, $E_v(x) = 500x$ meV, and $E_c(x) = 415 + 320x - 672x(1-x)$ meV]. We find that the unstrained $InAs_{0.1}Sb_{0.9}/InSb$ interface [Fig. 3(a)] has a type-II band alignment, while the $InAs/InAs_{0.9}Sb_{0.1}$ interface [Fig. 3(b)] has a type-I band alignment. To help understand these results, in Fig. 4 we plot E_c and E_v for unstrained $InAs_{1-x}Sb_x$ as functions of composition x. We see that the VBM energy always increases with Sb concentration, but the situation for the CBM is more complicated: There a minimum of E_c occurs at $x = 0.26$. For the Sb-rich alloy, the slope $dE_c/dx > 0$, so the CBM of unstrained $InAs_{1-x}Sb_x/InSb$ occurs on the layer with *lower* Sb concentration, and the alignment is clearly type II. This is illustrated schematically on the right-hand side of Fig. 4, showing the type-II band alignment of $InAs_{0.2}Sb_{0.8}/InSb$. On the other hand, for the As-rich condition $dE_c/dx < 0$, so the CBM of the unstrained $InAs/InAs_{1-x}Sb_x$ occurs on the layer with *higher* Sb concentration, and the system is expected to be type I. This is illustrated schematically on the left-hand side of Fig. 4, showing the type-I band alignment of $InAs/InAs_{0.8}Sb_{0.2}$.

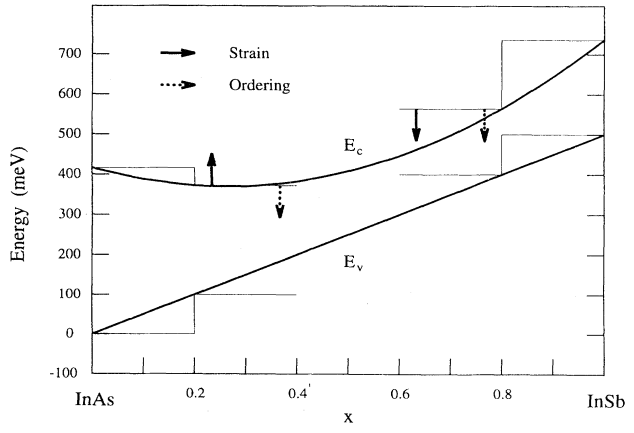

FIG. 4. The model variation of valence- and conduction-band-edge energies (in meV) as function of the InSb atomic concentration x for unstrained $InAs_{1-x}Sb_x$. We used our calculated valence-band offset $\Delta E_v(\text{InAs/InSb}) = 500$ meV, and attributed all of the band-gap optical bowing (Ref. 13) to the conduction band. Solid arrows indicate the effect of strain and dotted arrows show the effect of CuPt ordering.

C. Effects of strain on the offset between the pure compounds

For the biaxially compressed layer (InSb), the VBM is a heavy-hole (hh) $(\frac{3}{2},\pm\frac{3}{2})$ state, while for the biaxially expanded layer (InAs), the VBM is a light-hole (lh) $(\frac{3}{2},\pm\frac{1}{2})$ state.[27] From Fig. 2 we see the following strain-induced effects: (i) Under a 7% biaxial strain, the gap of InAs lattice matched to InSb is predicted to be *negative.* (ii) As in the unstrained case [Fig. 2(a)], the band alignment of the strained, *pure* InAs/InSb system [Figs. 2(b)–2(d)] is still type-II broken gap, with the CBM of InAs below the VBM of InSb. (iii) Mainly because of the crystal-field splitting at the top of the valence band, the InAs/InSb valence-band offset *increases* as the substrate lattice constant decreases: We find $\Delta E_v = 250$, 570, and 910 meV for $a_s = a(\text{InAs})$, $\bar{a}$, and $a(\text{InSb})$, respectively. It is interesting to note that experimentally extrapolated[24] *unstrained* valence-band offsets also follow this trend: the values obtained from Sb-rich heterostructures ($\sim$400 meV) (Refs. 2, 3, and 9) are smaller than that obtained[10] from As-rich heterostructures ($\sim$800 meV). (iv) Strain increases the conduction-band offset $\Delta E_c(\text{InAs/InSb})$ from 320 meV in the unstrained superlattice [Fig. 2(a)] to 680 meV in the (001) strained superlattices [Figs. 2(b)–2(d)].[28]

D. Effects of strain on the alloy interface

Assuming the same bowing parameter for the strained and unstrained alloys, the CBM energy of the strained alloy (independent of a_s) (Ref. 28) is given by $E_c(x) = E_c(0) + 680x - 672x(1-x)$ meV. In this strained alloy, $dE_c/dx > 0$ for all x, thus the *strained* $\text{InAs}_{1-x}\text{Sb}_x/\text{InAs}_{1-y}\text{Sb}_y$ heterostructure is always type II [Figs. 3(c) and 3(d)]. The increase of the conduction-band offset ΔE_c due to strain lowers the CBM energy of the As-rich layer relative to that in the Sb-rich layer. This effect of strain is denoted schematically by the heavy solid arrows in Fig. 4: in the Sb-rich (right-hand side) limit, strain *lowers* the CBM of the alloy, while in the As-rich (left-hand side) limit, strain *raises* the CBM of the alloy. In both cases, strain thus acts to enhance the type-II behavior. However, while the Sb-rich limit is already type II without strain (so that in this case strain *increases* the magnitude of ΔE_c), the As-rich limit is type I without strain, *so that strain diminishes ΔE_c, driving a type-I $\rightarrow$type-II transition.* We predict that, for InAs/$\text{InAs}_{1-x}\text{Sb}_x$ with $x < 0.5$, the system is type I for an unstrained superlattice, but changes to type II for a biaxially strained coherent (001) superlattice. However, in either the strained or unstrained case, the conduction-band offset for the As-rich interface is small [see Figs. 3(b) and 3(d)], indicating that the electrons in the corresponding superlattice will be quite delocalized.[12]

E. Effects of spontaneous ordering

Some of the $\text{InAs}_{1-x}\text{Sb}_x$ samples studied[5–8] exhibit spontaneous CuPt-type ordering in transmission electron microscopy (TEM). Ordering is known[4] to reduce the band gaps, primarily by lowering the CBM. Since we have just seen that strain in the As-rich alloys raises the CBM (thus driving a type-II offset), by lowering the CBM, ordering can thus drive a type-I offset. To estimate this effect, we recall that the band-gap reduction $\Delta E_g = E_g(\text{ordered}) - E_g(\text{random})$ can be expressed as[29]

$$\Delta E_g(\eta) = \Delta E_g(1)\eta^2 , \tag{6}$$

where $0 < \eta < \min[2x, 2(1-x)]$ is the order parameter and $\Delta E_g(1)$ is the ordering-induced band-gap reduction of the fully ordered ($\eta = 1$) alloy. From our first-principles band-structure calculation,[4] we find that $\Delta E_g(1) = 470$ meV for this system. Therefore, the maximum possible ordering-induced band-gap reduction for an $\text{InAs}_{1-x}\text{Sb}_x$ alloy at $x = 0.1$ is $\sim$19 meV (corresponding to $\eta_{\max} = 0.2$). Since the strained $\text{InAs/InAs}_{0.9}\text{Sb}_{0.1}$ system has a ΔE_c of only 8 meV [Fig. 3(d)], ordering could reverse the sign of ΔE_c, leading to a type-I offset. [Notice, however, that the large band-gap reduction observed in the MOCVD-grown sample ($\sim$60 meV for the $x = 0.1$ sample[6] and 28 meV for the $x = 0.07$ sample[7]) cannot be fully attributed to long-range ordering. As shown recently,[30] some of the band-gap reduction could be due to local phase separation in the samples.] Since alloy ordering universally *lowers* the energy of the CBM, ordering will enhance the type-II character in a Sb-rich $\text{InAs}_{1-x}\text{Sb}_x/\text{InSb}$ heterostructure. On the other hand, ordering will enhance the type-I character of an As-rich $\text{InAs/InAs}_{1-x}\text{Sb}_x$ heterostructure. These trends are illustrated by the dotted arrows in Fig. 4. It is thus possible that the MOCVD samples of Refs. 5–8 have stronger ordering and phase separation than the MBE samples of Refs. 9–12. Thus the former are type I, while the latter are type IIC.

V. SUMMARY

In summary, we find the following: (i) Pure InAs/InSb has a type-II broken gap alignment both with and without strain. (ii) For a Sb-rich InAsSb/InSb heterostructure, the unstrained band alignment is type II, and both epitaxial strain and CuPt ordering enhance the type-II character in this Sb-rich limit. (iii) For As-rich InAs/InAsSb heterostructures the top of the valence band is always on the alloy layer while the CBM can be localized either on the alloy layer (type I) or on the InAs layer (type II), depending on the balance between concentration, strain, and degree of ordering and phase separation. In this case, epitaxial strain enhances the type-II character, while ordering enhances the type-I character. For example, for $x < 0.5$ the system is type I if unstrained but type II if strained on InAs. Furthermore, the strained $\text{InAs/InAs}_{0.9}\text{Sb}_{0.1}$ system has ΔE_c of only $\sim$8 meV, so ordering and phase separation present mostly in the MOCVD samples can easily convert it to type I.[31]

ACKNOWLEDGMENTS

We thank A. Franceschetti for useful discussions. We also would like to thank R. A. Stradling, C. C. Phillips, S. R. Kurtz, and Y.-H. Zhang for discussion of their data prior to publication and for comments. This work was supported in part by the U.S. Department of Energy Grant No. DE-AC36-83-CH10093.

[1]G. C. Osbourn, J. Vac. Sci. Technol. B **2**, 176 (1984).
[2](a) S. R. Kurtz, G. C. Osbourn, R. M. Biefeld, L. R. Dawson, and H. J. Stein, Appl. Phys. Lett. **52**, 831 (1988); (b) S. R. Kurtz, G. C. Osbourn, R. M. Biefield, and S. R. Lee, *ibid.* **53**, 216 (1988).
[3]S. R. Kurtz and R. M. Biefeld, Phys. Rev. B **44**, 1153 (1991).
[4]S.-H. Wei and A. Zunger, Appl. Phys. Lett. **58**, 2684 (1991).
[5]S. R. Kurtz, L. R. Dawson, R. M. Biefeld, D. M. Follstaedt, and B. L. Doyle, Phys. Rev. B **46**, 1909 (1992).
[6]S. R. Kurtz, R. M. Biefeld, L. R. Dawson, K. C. Baucom, and A. J. Howard, Appl. Phys. Lett. **64**, 812 (1994).
[7]S. R. Kurtz, in Proceedings of the 7th International Conference on Narrow Gap Semiconductors, edited by J. Reno (AIP, New York, in press).
[8]S. R. Kurtz and R. M. Biefeld, Appl. Phys. Lett. **66**, 364 (1995).
[9]Y. B. Li, R. A. Stradling, A. G. Norman, P. J. P. Tang, S. J. Chung, and C. C. Phillips, in *Proceedings of the 22nd International Conference on Physics of Semicondutors,* edited by D. J. Lockwood (World Scientific, Singapore, 1994), p. 1496.
[10]M. J. Pullin, P. J. P. Tang, S. J. Chung, C. C. Phillilps, R. A. Stradling, A. G. Norman, Y. B. Li, and L. Hart, in Proceedings of the 7th International Conference on Narrow Gap Semiconductors (Ref. 7).
[11]Y. H. Zhang, Appl. Phys. Lett. **66**, 118 (1995).
[12]Y. H. Zhang, R. H. Miles, and D. H. Chow, IEEE J. Quantum Electron. (to be published).
[13]Z. M. Fang, K. Y. Ma, D. H. Jaw, R. M. Cohen, and G. B. Stringfellow, J. Appl. Phys. **67**, 7034 (1990), and references therein.
[14]R. H. Miles, D. H. Chow, J. N. Schulman, and T. C. McGill, Appl. Phys. Lett. **57**, 801 (1990).
[15]C. G. Van de Walle, Phys. Rev. B **39**, 1871 (1989).
[16]A. Qteish and R. J. Needs, Phys. Rev. B **45**, 1317 (1992).
[17]S.-H. Wei and A. Zunger, Phys. Rev. B **39**, 3279 (1989).
[18]G. Ji, S. Agurwala, D. Huang, J. Chyi, and H. Morkoc, Phys. Rev. B **38**, 10 571 (1988). These authors found a very large valence-band offset ($\sim$300 meV) in the $GaAs/GaAs_{0.9}Sb_{0.1}$ heterostructure. This value is considerably larger than the one found (Refs. 6–12) in $InAs/InAs_{0.9}Sb_{0.1}$ ($\sim$50–80 meV), and our theoretical calculation of Ref. 19, yielding $\sim$65 meV for unstrained heterostructure at $x=0.1$.
[19]P. Hohenberg and W. Kohn, Phys. Rev. **136**, B864 (1964); W. Kohn and L. J. Sham, *ibid.* **140**, A1133 (1965).
[20]D. M. Ceperly and B. J. Alder, Phys. Rev. Lett. **45**, 566 (1980).
[21]J. P. Perdew and A. Zunger, Phys. Rev. B **23**, 5048 (1981).
[22]S.-H. Wei and H. Krakauer, Phys. Rev. Lett. **55**, 1200 (1985), and references therein.
[23]S.-H. Wei and A. Zunger, Phys. Rev. Lett. **59**, 144 (1987); Phys. Rev. B **37**, 8958 (1988); J. Appl. Phys. (to be published).
[24]These experiments involve measurements on *strained* alloy heterostructures. They deduce the *unstrained* valence-band offset ΔE_v(InAs/InSb) using additional informations about the absolute deformation potential and bowing of the valence bands. This could introduce significant uncertainty in the derived value of the unstrained ΔE_v(InAs/InSb).
[25]S. Tiwari and D. J. Frank, Appl. Phys. Lett. **60**, 630 (1992).
[26]To test the assumption of attributing all of the bowing to the CBM, we have calculated the band-gap bowing coefficient b_g for $InAs_{1-x}Sb_x$ using the SQS-2 model [A. Zunger, S. H. Wei, L. G. Ferreira, and J. E. Bernard, Phys. Rev. Lett. **65**, 353 (1990)]. We find $b_g=650$ meV, in good agreement with experiment (Ref. 13). We next break $b_g=b_c-b_v$, using the core level as a reference. We thus estimated that the bowing for the valence band is $b_v=-130$ meV (i.e., it bows upwards). Including this nonzero valence-band bowing in Fig. 3 increases the alloy energy levels (both E_c and E_v) by $|b_v x(1-x)|=12$ meV. For As-rich heterostructure [Figs. 3(b) and 3(d)], this enhances its type-IIC character. Given the smallness of this change, we will assume $b_v=0$ in our following discussions.
[27]S.-H. Wei and A. Zunger, Phys. Rev. B **49**, 14 337 (1994) labeled the $(\frac{3}{2},\pm\frac{3}{2})$ state as the lh state and the $(\frac{3}{2},\pm\frac{1}{2})$ state as the hh state, according to the change of their in-plane effective mass under strain. In the present paper we adopted the more traditional labeling, i.e., denote the $(\frac{3}{2},\pm\frac{3}{2})$ state as the hh state and the $(\frac{3}{2},\pm\frac{1}{2})$ state as the lh state.
[28]The conduction-band offset ΔE_c is found to be independent of the substrate lattice constant. This is because the shift of the CBM energy is mainly due to the hydrostatic deformation potentials whose values are similar for InAs and InSb.
[29]S.-H. Wei, D. B. Laks, and A. Zunger, Appl. Phys. Lett. **62**, 1937 (1993); D. B. Laks, S.-H. Wei, and A. Zunger, Phys. Rev. Lett. **69**, 3766 (1992).
[30]K. A. Mader and A. Zunger, Appl. Phys. Lett. **64**, 2882 (1994).
[31]Our study does not include the quantum confinement effect which exists in thin superlattices. However, quantum confinement is limited by the depth of the well and, hence, is not expected to change the type of the band alignment.